Hard Limits and Performance Tradeoffs in a Class of Sequestration Feedback Systems

*Noah Olsman, *Ania-Ariadna Baetica, Fangzhou Xiao, Yoke Peng Leong, John C. Doyle, Richard M. Murray

November 20, 2017

Abstract

A common feature of both biological and man-made systems is the use of feedback to control their behavior. In this paper, we explore a particular model of biomolecular feedback implemented using a sequestration mechanism. This has been demonstrated to implement robust perfect adaptation, often referred to as integral control in engineering. Our work generalizes a previous model of the sequestration feedback system and develops an analytical framework for understanding the hard limits, performance tradeoffs, and architectural properties of a simple model of biological control. We find that many of the classical tools from control theory and dynamical systems can be applied to understand both deterministic and stochastic models of the system. Our work finds that there are simple expressions that determine both the stability and the performance of these systems in terms of speed, robustness, steady-state error, and noise. These findings yield a holistic picture of the general behavior of sequestration feedback, and will hopefully contribute to a more general theory of biological control systems.

1 Introduction

Natural biological circuits display a broad rage of feedback systems, often involving post-translational modification, gene regulation, and a variety of molecular and biochemical mechanisms [7, 8, 9, 12]. While these diverse architectures have been well-characterized in many systems, so far it has been difficult to analyze the general functions, constraints, and performance tradeoffs inherent to different feedback implementations. Recent work by Briat et al. made great strides in this direction by demonstrating that feedback mediated by sequestration can give rise to integral control, which in turn can implement robust perfect adaptation [4].

While integral control is a powerful tool, its stability and performance are not guaranteed to be well-behaved [2]. Even if both the controller and the plant (the network being controlled) are stable, their closed-loop dynamics can potentially be unstable, which results in poor regulation. Additionally, the closed-loop system performance indicates how well the controller performs the task of tracking a reference. Measures of performance include the tracking error, the speed of response, and the sensitivity. Further complicating the situation, noise and delay can impact the stability and performance of closed-loop control systems. To gain deeper insight into the system-level properties of biomolecular controllers, we will study the hard limits and tradeoffs of both the deterministic and the stochastic sequestration feedback system proposed in [4].

We find that there exists an analytic stability criterion for the linearized deterministic sequestration feedback system with an arbitrary number of simple first-order reactions in the plant. This stability criterion leads to a performance tradeoff between speed and sensitivity in the system - fast responding controllers are intrinsically more fragile. These results are analyzed both in the case where there is no controller degradation (as in the model from [4]) and in the more biologically-realistic context where there is such degradation [15], where we observe yet another tradeoff between stability and steady-state

*Equal contribution

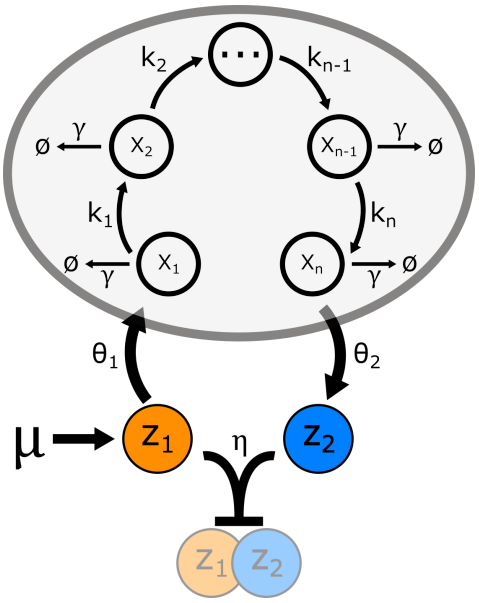

Figure 1: A Sequestration Feedback Architecture. This diagram shows an example of a fundamental sequestration feedback network. This general model has two control species, Z_1 and Z_2, and n plant species. Within this model is a simple set of possible plants where each species is only involved in the production of the next species. This model is useful because it not only is able to capture the complexity of a system with many species, but it also is simple enough to study analytically.

error. Finally, we demonstrate a close theoretical correspondence between stability in the deterministic model of sequestration feedback and variance in a simplified stochastic model of the system. These results provide a more precise framework for understanding the system-level properties of biomolecular controllers.

These general theoretical results will provide an analytical framework to study many particular implementations of biological control architecture, while maintaining a broad perspective regarding how they relate to each other. For instance, we can begin to study the performance tradeoffs between a controller implemented at different biological layers (e.g., genes, RNA, or proteins). Section 2.1 describes the model of the system and reviews basic results about integral control. Similar limits have been studied in the context of general stochastic biological control systems [13] and in the particular context of the control in the yeast glycolysis system [5]. Section 2.2 and Section 2.3 use control theoretic tools to analyze performance in the sequestration feedback system. Section 3 considers the biological implementation of the controller architecture. Section 3.1 incorporates the controller species degradation into the model. Section 3.2 discusses the stability of the network. Section 3.3 derives an optimal controller degradation rate. Section 4 clarifies the connection between the stability margin of the deterministic controller and the variance of the stochastic controller output.

2 Results for a Simple Deterministic Model

This section presents a few interesting results for a simple sequestration feedback model proposed by Briat et al. with two control states and two plant states. The stability of this feedback network is analyzed, and fundamental tradeoff between the species' production rates and the network's robustness with respect to external disturbances is described.

2.1 Model Description

We first describe the simple sequestration feedback model proposed by Briat *et al.* with two control states (z_1 and z_2) and two plant states (x_1 and x_2), which corresponds to the general diagram in

Figure 1 if $n = 2$. The biochemical reactions of the sequestration network with two plant species are the following:

$$\emptyset \xrightarrow{\mu} Z_1 \qquad Z_1 \xrightarrow{\theta_1} Z_1 + X_1 \qquad X_1 \xrightarrow{k} X_2 \qquad X_2 \xrightarrow{\theta_2} X_2 + Z_2$$
$$X_1 \xrightarrow{\gamma} \emptyset \qquad X_2 \xrightarrow{\gamma} \emptyset$$
$$Z_1 + Z_2 \xrightarrow{\eta} \emptyset.$$

Formally, their model is given as:

$$\dot{x}_1 = \theta_1 z_1 - \gamma x_1, \tag{1a}$$
$$\dot{x}_2 = k x_1 - \gamma x_2, \tag{1b}$$
$$\dot{z}_1 = \mu - \eta z_1 z_2, \tag{1c}$$
$$\dot{z}_2 = \theta_2 x_2 - \eta z_1 z_2. \tag{1d}$$

The variables θ_1 and θ_2 are production rates that provide an interface between the plant and the controller. The variable θ_1 is the production rate of the input of the plant (x_1) that is affected by the output of the controller (z_1), and the variable θ_2 is the production rate the input of the controller (z_2) that is affected by the output of the plant (x_2). The rates k and γ are production and degradation rates that are internal to the plant species. An external reference μ determines production of z_1, and the two control species z_1 and z_2 sequestrate at the rate of η.

While more realistic models of biological circuits will have more complex interactions and likely have many more states, this model captures much of the important structural information about the sequestration feedback system. In particular, Briat *et al.* found that the network defined by (1) implements precise adaptation of x_2 via integral feedback [4], as shown by the following relationship

$$\dot{z}_1 - \dot{z}_2 = \mu - \theta_2 x_2 \implies (z_1 - z_2)(t) = \theta \int_0^\infty \left(\frac{\mu}{\theta_2} - x_2(t') \right) dt'. \tag{2}$$

This relationship ensures that, *if* the system is stable, then at steady state, $x_2 = \mu/\theta_2$. However, conditions that guarantee stability are not obvious at first glance. Briat *et al.* showed general algebraic conditions that proved existence of both stable and unstable dynamics of the linearized sequestration feedback system, however it is not obvious how to use their methods to explicitly describe stability in general.

In this paper, we show that there exist particular limits (for example, strong feedback) for which we can prove what the stability criterion is in closed form. Later, we will show that a one-state plant is intrinsically stable for all parameters, and that there exists a simple stability criterion for a certain class of plants with two or more states. For the analysis, we assume that both a set of plant parameters (k and γ) and a desired set point (determined by μ and θ_2) are given, and we study how stability and performance relate to the rest of the control parameters (θ_1 and η).

2.2 Linear Stability Analysis

A key difficulty in studying the sequestration feedback is the nonlinear term $\eta z_1 z_2$ that mediates feedback in Equations (1c) and (1d). While there exist techniques to study nonlinear systems, there are far more general tools available to study linear systems. To this end, we will study instead the linearization of the sequestration feedback system, which has the form

$$\begin{bmatrix} \dot{x}_1 \\ \dot{x}_2 \\ \dot{z}_1 \\ \dot{z}_2 \end{bmatrix} = \begin{bmatrix} -\gamma & 0 & \theta_1 & 0 \\ k & -\gamma & 0 & 0 \\ 0 & 0 & -\beta & -\alpha/\beta \\ 0 & \theta_2 & -\beta & -\alpha/\beta \end{bmatrix} \begin{bmatrix} x_1 \\ x_2 \\ z_1 \\ z_2 \end{bmatrix}, \tag{3}$$

where $\alpha = \theta_1 \theta_2 k/\gamma^2$ and $\beta = \eta\mu$. From simulations (see Section 6.1), we find that the linearized model well approximates the nonlinear one. The main distinction is that each variable in the nonlinear model

remains positive at all times and cannot grow in an unbounded way. This distinction is primarily apparent when the system is unstable: the linear system simply grows forever while the nonlinear system simply oscillates indefinitely.

In general, stability of linear systems is determined by the sign of the real part of its eigenvalues. If they are all strictly negative, then the dynamical system is stable and the system will converge to the equilibrium point. Ideally, we would be able to directly compute the eigenvalues of the matrix

$$M = \begin{bmatrix} -\gamma & 0 & \theta_1 & 0 \\ k & -\gamma & 0 & 0 \\ 0 & 0 & -\beta & -\alpha/\beta \\ 0 & \theta_2 & -\beta & -\alpha/\beta \end{bmatrix},$$

however this computation corresponds to finding the roots of a fourth-order polynomial $p(s) = \det(sI - A)$. While this is difficult to do in general, it is possible to study stability by finding what has to be true of the parameters for the system to have a pair of purely imaginary eigenvalues, which characterizes the boundary between stable and unstable behavior. We find that, in the limit of strong feedback (i.e. η large), M will have purely imaginary eigenvalues $\lambda = \pm i\gamma$ when $\gamma = \sqrt[3]{\frac{\theta_1\theta_2 k}{2}}$. We can then show that the criterion for stability is

$$\sqrt[3]{\frac{\theta_1\theta_2 k}{2}} < \gamma, \tag{4}$$

a relationship we refer to as the production-degradation inequality. This result is proved in Section 6.2.

This relationship says that the closed-loop system will be stable so long as the degradation rate is larger than a constant that is proportional to the geometric mean of the production rates ($\sqrt[3]{\theta_1\theta_2 k}$). In simpler terms, stability relies on the degradation rate out-pacing the mean production rate. We note that in this strong feedback limit, Equation (4) is independent of the controller variables μ and η. Thus, this relationship tells us that stability is purely a function of the parameters describing the plant and its connection to the controller, and is independent of the controller itself. Intuitively, the degradation rate sets the rate of adaptation of x_1 and x_2, so Equation (4) tells us that, so long as the species have a rate of adaptation that is faster than the rate of change in production, the system will be stable. Through a more technical argument (also in Section 6.2), we can show that an analogous system with a chain of n plant species has a production-degradation inequality of the form

$$\sqrt[n+1]{\frac{\theta_1\theta_2\prod_{i=1}^{n-1} k_i}{\Delta_n}} < \gamma,$$

where Δ_n is a constant that is only a function of the number of plant species. When the system has purely imaginary eigenvalues, they have the form

$$\lambda = \pm i \tan\left(\frac{\pi}{2n}\right)\gamma.$$

Finally, for simplicity, we focus only on the strong feedback regime. However, we show in the supplement that there are also tractable and interesting results in the regime of weak feedback (η small). The results have a similar form as in the strong feedback limit, however the difference in assumption of the feedback strength flips the direction of the inequality. The stability condition for weak feedback is:

$$\sqrt[n-1]{\frac{\Delta_n\theta_1\theta_2\prod_{i=1}^{n-1} k_i}{\beta}} > \gamma.$$

One interpretation of these results as a whole is that stability occurs when either feedback *or* plant degradation are sufficiently large, but not when both are.

2.3 Performance Tradeoffs and Hard Limits

While Equation (4) gives us a binary condition to classify stability, it tells us little about overall performance of the system. We know when the system becomes unstable, but it is unclear how the

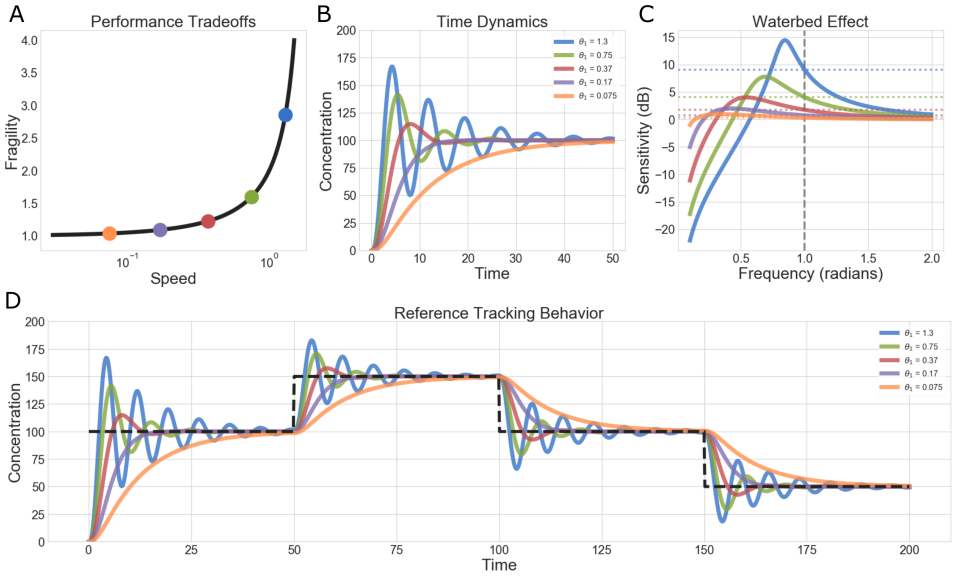

Figure 2: Speed/Fragility Tradeoff. **A)** We see the relationship between speed and fragility in the sequestration feedback system. Speed can be characterized in terms of any of the production rates of the system, here we vary θ_1, where higher production rates lead to a faster response. Fragility is defined as a lower bound on the maximum value of the sensitivity function $\|S\|_\infty$. **B)** Time-domain plots corresponding to different points on the tradeoff curve in **A**. We see that speed and fragility naturally relate to the rise time and settling time of the system. **C)** Sensitivity functions for various parameter values. We see what is known in control theory as a waterbed effect, where better attenuation of disturbances at low frequencies necessarily implies worse amplification of disturbances at higher frequencies. Dotted lines correspond to the lower-bounds on the sensitivity function that can be analytically computed for use in panel **A**. **D)** Reference tracking dynamics, analogous to the simulations shown in **B**. In these simulations θ_1 is varied and $k = \theta_2 = \gamma = 1$, $\eta = 10^5$, $\mu = 100$ unless otherwise specified.

system behaves as it approaches instability. Conversely, we can increase the margin of stability by decreasing the production rates θ_1, θ_2, and k, but this will slow down the dynamics of the system and could potentially hurt performance.

To analyze this problem, we will study the sensitivity function $S(s)$, which is the transfer function between the output of the system and disturbances [2]. This transfer function captures the amplification of external disturbances on the output of a system, in this case, x_2. A system is termed robust if the system output is not strongly affected by the external disturbances. Thus, S provides a way to quantify system robustness. It is often useful to study $S(s)$ in the frequency domain, *i.e.* when $s = i\omega$. When $|S(i\omega)| > 1$, a periodic disturbances with frequency ω will be amplified, when $|S(i\omega)| < 1$ then they will be attenuated. Ideally all unwanted disturbance would be rejected (*i.e.* attenuated). However, a classical result known as Bode's integral theorem states that for any closed-loop control system,

$$\int_0^\infty |\log(S(i\omega))| d\omega \geq 0,$$

which means that the total magnitude of S at all frequencies is bounded below by 0 [2]. In other words, if we wish to better attenuate disturbances at one frequency (decrease $|\log(S(i\omega_1))|$ at ω_1), they must be amplified somewhere else (increase $|\log(S(i\omega_2))|$ at ω_2). This effect is often referred to in control theory as a waterbed effect, since pushing down on one part of S necessarily causes a rise somewhere else.

The robustness of a system can be formally quantified with $\|S\|_\infty = \max_\omega |S(i\omega)|$, the maximum magnitude of the sensitivity function across all frequencies. The quantity $\|S\|_\infty$ can be thought of as a measure of the robustness of the system, because it tells us how bad the worst-case disturbance is

for the system. If $\|S\|_\infty$ is in some sense small enough to be manageable, then values of $|S|$ across all frequencies are also small and the system is robust to any disturbance. If $\|S\|_\infty$ is large enough to be a problem, then there is at least one disturbance against which the system is fragile.

Directly computing $\|S\|_\infty$ in terms of the parameters of a system is difficult in general, but it is sometimes possible to compute good lower bounds that yield insight into a systems robustness. To this end, we find that (see Section 6.3 for details):

$$\|S\|_\infty \geq \frac{1}{1 - \frac{\theta_1\theta_2 k}{2\gamma^3}}, \tag{5}$$

with equality when

$$\gamma = \sqrt[3]{\frac{\theta_1\theta_2 k}{2}} \implies \frac{\theta_1\theta_2 k}{2\gamma^3} = 1 \implies \|S\|_\infty = \infty.$$

Finally, Figure 2D shows reference tracking to step inputs for the system. We see again that there is a tradeoff between speed and fragility as we move along different points in parameter space.

A key structural aspect of the model described so far is that z_1 and z_2 are only removed from the system via sequestration. This is what ensures the precise adaptation in Equation (2). If the control molecules also undergo intrinsic degradation of their own, the controller will not necessarily exhibit perfect integral feedback. In the next section, we will explore what changes in the system when controller species degradation is present.

3 The Implementation of Sequestration Feedback Networks

Sequestration feedback networks can be implemented using an array of biological parts for the two sequestering controller species. Several examples of parts for the two controller species are illustrated in Figure 3. They include transcriptional parts such an mRNA-antisense RNA pair, protein parts such a sigma-antisigma pair or a toxin-antitoxin pair, or a protein and an enzyme, such as a scaffold protein and a kinase.

Transcriptional parts can be obtained from natural systems such as the hok-sok Type I toxin-antitoxin system in the *E. coli* or from parts already mined for synthetic biological systems. The hok gene product is a toxin that kills cells without its antidote, the anti-sense RNA sok that is complementary to the hok mRNA [10]. A synthetic system of RNA-antisense RNA that originally performed translation initiation control is adapted to regulate transcriptional elongation in [14]. Protein parts can be obtained from Type II toxin-antitoxin bacterial systems such as CcdA/CcdB. The toxin CcdB targets DNA gyrase and induces the breaking of DNA and subsequently cell death, while its antitoxin CcdA inhibits CcdB toxicity by sequestering it into a very stable CcdA-CcdB complex [6]. Protein parts can also be sigma-antisigma factors such as $\sigma 70$ binding to bacteriophage T4 AsiA and inhibiting RNA polymerase, which slows transcription and inhibits *E. coli* growth [16]. Lastly, sequestration controller parts could be scaffold proteins, such as the synthetic scaffold and anti-scaffold proteins in [11]. The scaffold molecule consists of a leucine zipper domain (LZx) linked to the SH3 ligand; the anti-scaffold consists of the complementary LZx and SH3 ligand domains, which allows the two to bind tightly.

Depending on the choice of parts for the controller species in sequestration feedback networks, the binding affinity of the sequestration reaction can vary over several orders of magnitude, as illustrated in Figure 3. However, as discussed in Section 2, the binding affinity of the sequestration feedback influences the stability of the sequestration feedback network. Therefore, we need to carefully consider whether our implementation choice for the controller parts results in stable closed loop control.

Additionally, depending on the implementation parts for the sequestration binding, the degradation rates of the controller species can vary, as illustrated in Table 1. The degradation rate of mRNA or $\sigma 32$ is small and can even be omitted in our modeling of the sequestration feedback network [1], unless the controller species are also actively degraded. However, the degradation rate of the toxin and anti-toxin is non-trivial and must be included in the model.

To recover near-perfect adaptation in the presence of non-trivial controller degradation rate, Qian et al. propose a time-scale separation between the controller reactions and dilution [15]. In this section,

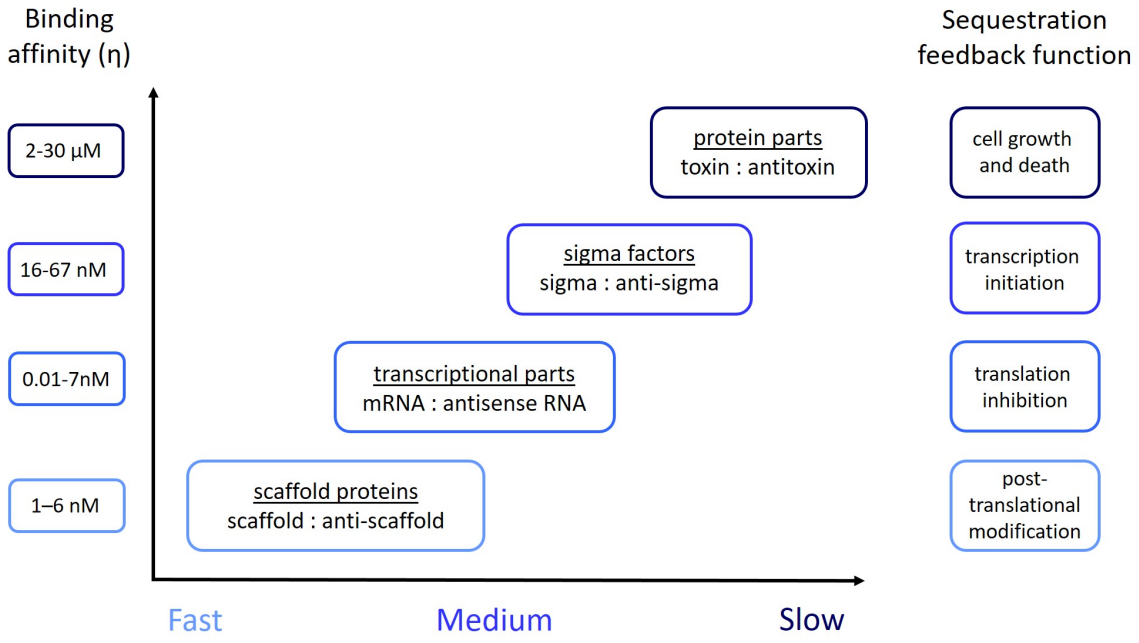

Figure 3: The Biological Implementation Of The Sequestration Reaction. The controller sequestration reaction can be implemented with a multitude of biological parts. Example transcriptional parts are mRNA and antisense RNA, whose kinetic binding affinity is calculated in [18]. Antisense RNA inhibits the translation of complementary mRNA by base pairing to it and physically obstructing the translation machinery of the cell. Antisigma factors bind sigma factors to inhibit transcriptional activity; sigma-antisigma factors binding affinity was computed in [16]. Protein parts include the toxin-antitoxin module CcdA-CcdB in E. coli. When CcdB outlives CcdA, it kills the cell by poisoning DNA gyrase. The antitoxin CcdA blocks the activity of the toxin CcdB by binding together into a complex, thus allowing cells to grow normally. Their binding affinity is very high [6]. Scaffold parts include the synthetic scaffold consisting of leucine zipper domain (LZX) linked to the SH3 ligand and the anti-scaffold consisting of the complementary LZx and SH3 ligand domains. Their binding affinity is given in [11].

mRNA	$\sigma 32$	CcdA	CcdA:CcdB
2.1-6 min	1 min	30 min	60 min

Table 1: The half-life of mRNA, sigma factor $\sigma 32$, antitoxin CcdA, and toxin-antitoxin complex CcdA-CcdB. The median mRNA half-life is measured as 2.1-6 min in [3]. The half-life of $\sigma 32$ factor proteins during steady-state growth is 1min [8]. The antitoxin CcdA is degraded in wild-type cells with a half-life of 30 min in the absence of toxin CcdB and a half life of 60 min in the presence of toxin CcdB [17].

we perform a general analysis of the stability and the performance of sequestration feedback systems and we discuss how it informs our choices of biological implementation.

3.1 The Sequestration Feedback Network Model with Controller Species Degradation

We assume that the controller species are subjected to degradation with rate γ_c, while the plant species are degraded with rate γ_p. Therefore, the chemical reactions that describe the sequestration feedback

network are modified from Figure 1 to the following

$$\emptyset \xrightarrow{\mu} Z_1, \qquad Z_1 \xrightarrow{\theta_1} Z_1 + X_1, \qquad X_n \xrightarrow{\theta_2} X_n + Z_2,$$
$$X_i \xrightarrow{\gamma_p} \emptyset, \quad \forall 1 \leq i \leq n, \qquad Z_1 \xrightarrow{\gamma_c} \emptyset, \qquad Z_2 \xrightarrow{\gamma_c} \emptyset,$$
$$Z_1 + Z_2 \xrightarrow{\eta} \emptyset.$$

When we incorporate the degradation of the controller species in the model, the description changes the controller Equations (1c), (1d) to the following:

$$\begin{aligned} \dot{z}_1 &= \mu - \eta z_1 z_2 - \gamma_c z_1, \\ \dot{z}_2 &= \theta_2 x_2 - \eta z_1 z_2 - \gamma_c z_2. \end{aligned} \tag{6}$$

The sequestration feedback networks with and without controller degradation have different properties of stability and performance. First, the stability margins of the sequestration feedback network with and without controller degradation can be tuned differently. While the stability margin of the sequestration feedback network with no controller degradation can be improved by increasing the plant degradation rate, the stability margin of the sequestration feedback network with controller degradation can be improved by increasing either the plant or the controller degradation rates. Additionally, the stability criterion for the sequestration feedback network with controller degradation has a different form, dependent on comparing the plant degradation rate and the controller degradation rate, as discussed in Section 3.2.

Secondly, we consider how the controller species degradation rates influence the steady state error of the sequestration feedback system. A stable sequestration feedback system with small controller species degradation, such as for mRNA and sigma factor, implements near-perfect adaptation, which implies close to zero steady state error. However, a sequestration feedback system with controller species degradation rate on the order of cell dilution, such as for toxin and scaffold proteins, has a steady state error that is sensitive to the controller degradation rate. In fact, there is a unique critical value of the controller degradation rate that recovers the property of zero steady state error, as demonstrated in Figure 4. We analytically derive the unique controller degradation rate that recovers the property of zero steady state error in Section 3.3.

Finally, we uncover a tradeoff between the stability margin and the steady state error in sequestration feedback systems in Section 3.4. Increasing either the plant or the controller species degradation rate improves stability, but this can result in poor steady state error. We find that the steady state error is more sensitive to changes in the plant species degradation rate than the controller species degradation rate. Therefore, we have more options to tune the controller species without negatively impacting the sequestration feedback system's performance.

3.2 Stability Analysis

The criterion for the stability of sequestration feedback networks with controller degradation is obtained by comparing the plant degradation rate γ_p and the controller degradation rate γ_c. We consider three possible comparisons between the plant degradation rate and the controller degradation rate: $\gamma_p >> \gamma_c$, $\gamma_p \approx \gamma_c$, and $\gamma_p << \gamma_c$.

The comparison between the plant and the controller species degradation rates is motivated by their ratio of the two degradation rates appearing as a term in associated the characteristic polynomial:

$$(s+1)^n \left(s + \frac{\gamma_c}{\gamma_p}\right)\left(s + \frac{\gamma_c}{\gamma_p} + \frac{\alpha + \frac{\beta}{\alpha}}{\gamma_p}\right) = -\frac{\beta}{\gamma_p^2} \tag{7}$$

The value of the ratio of the plant and the controller degradation rates informs the location of the complex roots of the characteristic polynomial.

We formalize the stability criterion in Theorem 3.1 below and we include the derivation in the supplement, Sections 6.6 and 6.7.

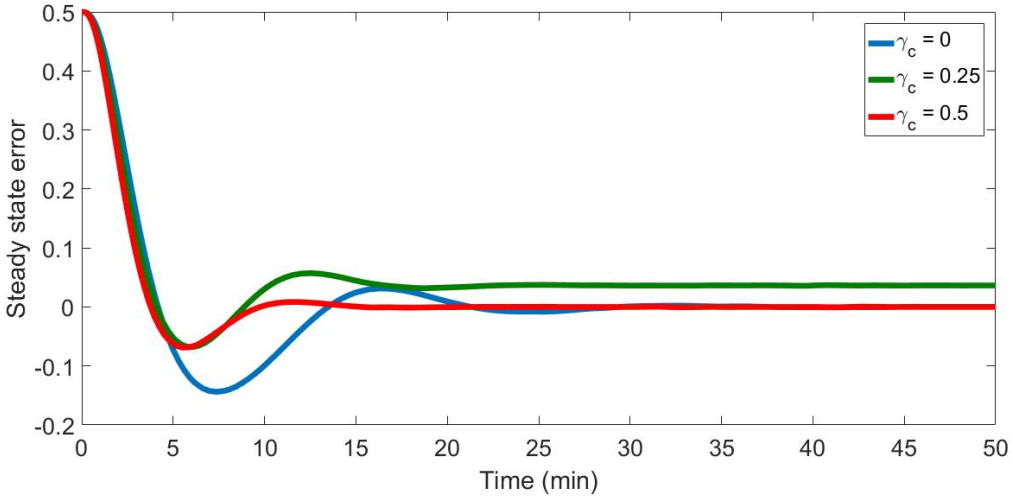

Figure 4: Controller Degradation And Steady State Error. When $\gamma_c = 0$, there is no controller degradation and therefore the sequestration feedback network exhibits perfect adaptation (blue). Therefore, the output converges to the reference with zero steady state error. When the controller degradation rate is $\gamma_c = 0.25$, the sequestration feedback network has non-zero steady state error (green). However, when the controller degradation rate is $\gamma_c = 0.5$, the sequestration feedback network once again displays the property of zero steady state error (red). Indeed, the degradation rate values $\gamma_c \in \{0, 0.5\}$ are the only ones for which the network output tracks the reference with zero steady state error.

Theorem 3.1. *We consider the sequestration feedback network with controller degradation described in Equation (6) under the strong feedback assumption. The closed loop stability criterion depends on the relationship between the plant degradation rate γ_p and the controller degradation rate γ_c. We consider the following three cases:*

Case I: *$\gamma_c \ll \gamma_p$ If the controller's degradation rate is much smaller than the plant's degradation rate, the stability criterion is the same as the production-degradation inequality in Section 2.2.*

Case II: *$\gamma_c \approx \gamma_p$ If the controller's and plant's degradation rates are comparable in magnitude, then the closed loop system is stable under the following conditions:*

$$\begin{aligned} &\gamma_c \approx \gamma_p, \\ &\gamma_p > \frac{\sqrt[n+1]{\theta_1\theta_2\prod_{i=1}^{n-1} k_i}}{\sqrt{\tan(\frac{\pi}{n+1})^2 + 1}}. \end{aligned} \tag{8}$$

Case III: *$\gamma_c \gg \gamma_p$ If the controller's degradation rate is larger than the plant species' degradation rate, then the closed loop system is stable if*

$$\begin{aligned} &\gamma_c \gg \gamma_p, \\ &\gamma_p > \frac{\sqrt[n]{\theta_1\theta_2\prod_{i=1}^{n-1} k_i}}{\sqrt[n]{\gamma_c}\sqrt{1 + \tan\left(\frac{\pi}{n}\right)^2}}. \end{aligned} \tag{9}$$

First, when the plant degradation rate is much larger that the controller degradation rate, then the ratio of the two degradation rates approaches value zero and the stability criterion is the same as in the production-degradation inequality in Section 2.2. Secondly, when the plant degradation rate is comparable to the controller degradation rate, then the ratio of the two degradation rates approaches value one and the stability criterion states that the plant degradation be faster than the product of its production rates. Lastly, when the plant degradation rate is much smaller than the controller degradation rate, then the ratio of the two degradation rates is very large and the stability criterion

states that the plant degradation be faster than the product of its production rates divided by the controller degradation rate.

3.3 The Critical Controller Degradation Rate

When the controller degradation is negligible, then the sequestration feedback network exhibits the property of perfect adaptation. The controller species implement integral control, which ensures that the steady state error equals zero, provided that the closed loop system is stable.

When the controller degradation rate is not negligible, as in Table 1, we need to include it in the model for the sequestration feedback network. In this case, the closed loop system has zero steady state error only for a unique value of the controller degradation rate, which we call the critical controller degradation rate.

In the supplement, Section 6.5, we analytically derive the critical controller species degradation rate such that the steady state error of a general sequestration feedback network with n plant species equals zero. We also derive conditions such that the critical controller degradation rate is achievable by the network parameters and we demonstrate that it is unique. Here we only include the analytical result for a cyclical plant network.

Theorem 3.2. *The critical controller degradation rate for a cyclical plant network (i.e. each plant species X_i is created by the previous plant species X_{i-1} and creates the next plant species X_{i+1}, $\forall 2 \leq i \leq n-1$, as in Figure 1) is given by:*

$$\gamma_c = \frac{\theta_1 \theta_2 \prod_{i=1}^{n-1} k_i}{\gamma_p^n} - \frac{\eta \mu \gamma_p^n}{\theta_1 \theta_2 \prod_{i=1}^{n-1} k_i}. \tag{10}$$

It can only be achieved if and only if

$$\gamma_p < \sqrt[n]{\frac{\theta_1 \theta_2 \prod_{i=1}^{n-1} k_i}{\sqrt{\eta \mu}}}. \tag{11}$$

We illustrate the effect of the controller degradation rate for a two-plant network in Figure 4. When the controller degradation rate is negligible, then the steady state error equals zero (blue). Similarly, at the critical controller degradation rate, the steady state error also equals zero (red). Indeed, the degradation rate values of zero and of the critical degradation rate are the only ones for which the network tracks the reference with no steady state error.

3.4 The Steady State Error and the Stability Margin

Even if the optimal value of the controller species degradation rate γ_c can be achieved mathematically, it can not be implemented exactly in a biological system. Hence, a more interesting question is how sensitive the steady state error and the stability margin are to the controller degradation rate. We also compare their sensitivity to the controller species degradation rate versus sensitivity to the plant species degradation rate.

It is clear from our derivation of stability criteria that increasing either γ_p or γ_c has a beneficial effect of increasing the stability margin (see supplement, Section 6.6). However, increasing γ_c or γ_p can result in a poor steady state error, as illustrated in Figure 5A. Therefore, there is a tradeoff between stability margin and low steady state error.

Additionally, Figure 5A indicates that the steady state error is more sensitive to changes in the plant species degradation rate than in the controller species degradation rate. Therefore, we have more freedom to tune the controller species degradation rate without negatively impacting the network's performance.

Figure 5 suggests that a robust implementation of sequestration feedback networks uses a medium to high degradation rate of the plant species, while allowing for a range of controller species degradation rate values. According to Figure 3, one such implementation choice uses proteins parts for both the plant and the controller species. We assume that there is no active degradation of these protein

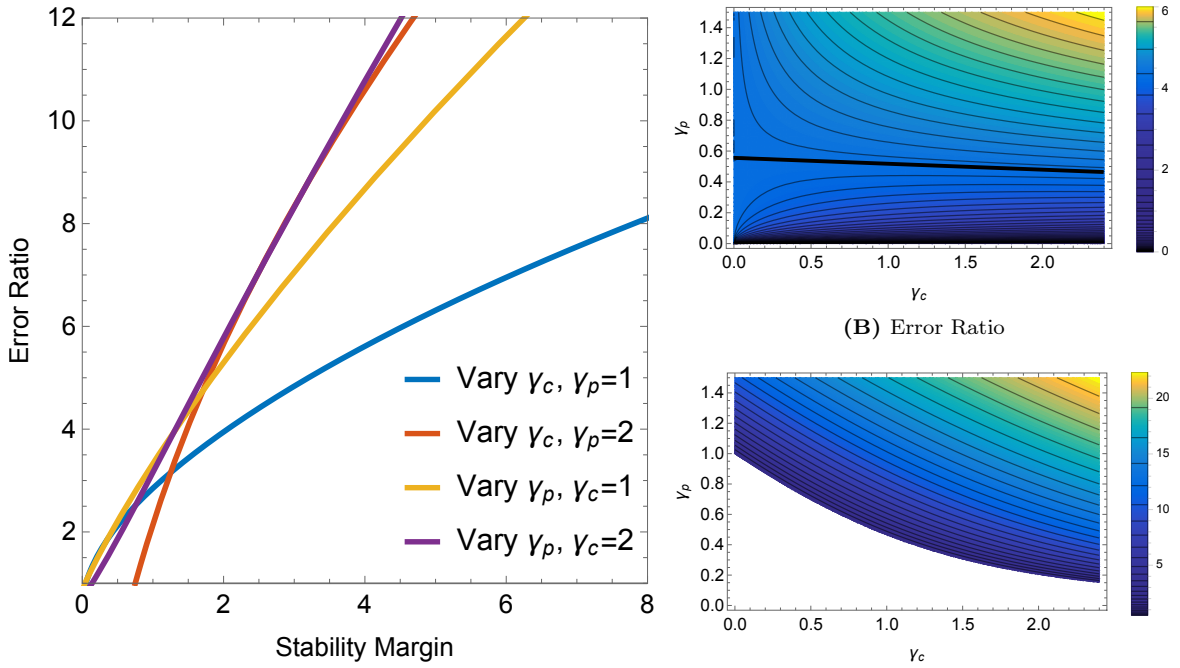

(A) Tradeoffs

(B) Error Ratio

(C) Stability Margin

Figure 5: Stability Margin/Error Tradeoff. There is a tradeoff between good stability margin and low steady state error in the sequestration feedback network with controller degradation. A. Increasing either the plant species degradation rate γ_p or the controller species degradation rate γ_c improves the stability margin. However, varying the plant species degradation rate γ_p results in a worse tradeoff than varying the controller species degradation rate γ_c because the error ratio is more sensitive to the plant species degradation rate γ_p than the controller species degradation rate γ_c. B. The thick black line indicates no error (*i.e.* the ratio between the steady state error and the reference is one). It is clear from this plot that changing γ_p by a small amount will deviate from the black line significantly more than changing γ_c by a small amount. C. The white region is unstable. Increasing either γ_p or γ_c will improve stability margin.

species. Then the plant and controller degradation rates will match the cell growth rate. A less robust implementation is to use RNAs for the plant species and proteins for the controller species. Then the plant species will have high turnover, whereas the controller species will dilute more slowly with cell growth. In this implementation, choosing the appropriate cell growth rate and cell growth medium will be of importance as the sequestration feedback's performance will be sensitive to the plant and controller species degradation rate.

4 Stochastic Sequestration Feedback Networks

We connect the deterministic and stochastic sequestration feedback systems by examining the stability of deterministic sequestration feedback systems and the second moment of the output species of stochastic sequestration feedback systems. Our results complement and expand on the stochastic analysis in Briat et al. [4].

Our analysis is motivated by the performance of the stochastic sequestration feedback controller, which can be slow or noisy, as illustrated by the coefficient of variation of the output species in Figure 6B, C. Slow transient dynamics are time consuming and stochastic noise can be amplified by connecting multiple controllers. Therefore, stochastic controllers should be fast and not very noisy, as the illustrated in Figure 6A.

To connect deterministic and stochastic sequestration feedback systems, we derive an analytical expression for the steady state mean and variance of the output species in a stochastic sequestration feedback system with two plant species. We clarify the role of the second moment in informing the

stability and performance of the closed loop stochastic sequestration feedback system. Additionally, we demonstrate that only considering the first moment does not suffice to obtain good stochastic controller properties. Indeed, the stochastic mean can be ergodic and well-behaved, while individual stochastic trajectories are noisy or even oscillatory. This can occur when individual trajectories oscillate with random frequencies that average out in the mean, as in Figure 7.

We also illustrate that the stability of deterministic sequestration feedback systems corresponds to the size of the variance of the stochastic sequestration feedback system. The stability margin of the deterministic sequestration feedback system appears in the denominator for the expression of the Fano factor. Therefore, if the plant species degradation rate is small, the stochastic variance grows large and the deterministic sequestration feedback system approaches instability.

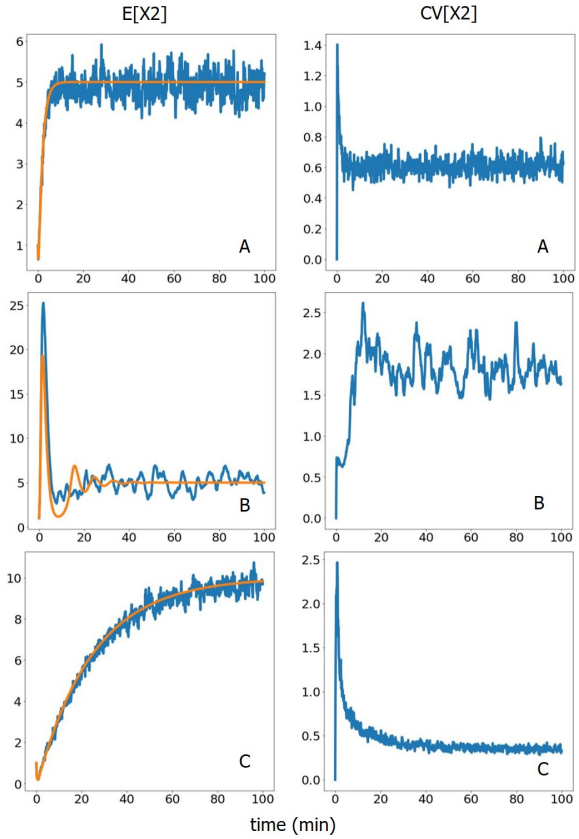

Figure 6: Stochastic Controller Performance. The stochastic control objective is that the sequestration network output species tracks the reference value $\frac{\mu}{\theta} = 5$. In panels A-C, the left hand plots are the mean of X_n across a population of 1000 independent cells as a function of time (blue-stochastic, orange-deterministic); the right hand plots are the coefficient of variation (i.e. the ratio of the standard deviation to the mean) across the cell population as a function of time. Panel A: the controller performance is good. Panel B: the controller is very noisy. Panel C: the controller is slow. Poor stochastic controllers are noisy and have slow dynamics.

4.1 The First Two Moments of the Stochastic Feedback Network Output

We first demonstrate how averaging out individual stochastic trajectories often results in a well-behaved stochastic population mean, as discussed in Briat et al. [4]. In Figure 7A, B, the output of the deterministic sequestration feedback system and the mean of the output of the stochastic sequestration feedback system converge to the reference quickly, with damped oscillations. In Figure 7A, the individual stochastic trajectories are not very noisy; however, the noise increases in Figure 7B.

In contrast, the stochastic controller is well-behaved in the mean output across a set of trajectories, but noisy and oscillatory at the individual trajectory level in Figure 7C. This occurs because the

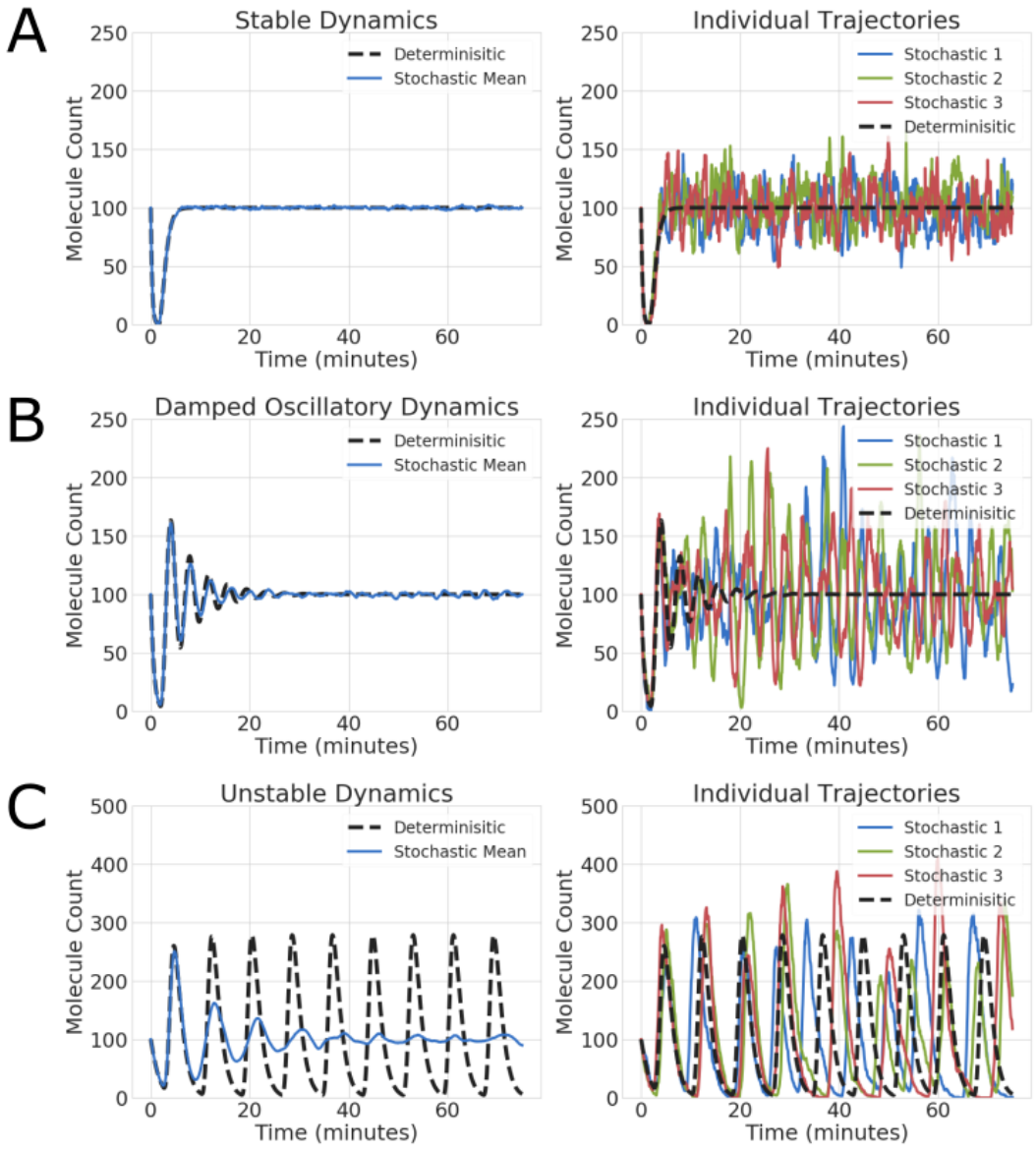

Figure 7: Averaging Stochastic Trajectories. We illustrate how averaging individual stochastic trajectories results in a well-behaved stochastic population mean. Even if the stochastic population mean is finite and converging as a function of time, individual stochastic trajectories can be very noisy and oscillatory. A. The deterministic and stochastic mean converge with good performance; individual stochastic trajectories are not very noisy. B. The deterministic and stochastic mean have damped oscillations; individual stochastic trajectories are noisy. C. The deterministic model oscillates; the stochastic mean has damped oscillations, as demonstrated in [4]; however, the individual trajectories oscillate.

individual trajectories oscillate, but with random frequencies that average out when we compute the stochastic mean. Thus, the population mean of the stochastic model does not match the controller performance for individual trajectories and higher order moments must be considered. This motivates our interest in the Fano factor as a quantity that better captures the stochastic controller's noise properties.

4.2 Deterministic and Stochastic Feedback Systems

To explore the connection between deterministic and stochastic sequestration feedback control, we derived an expression for the steady state Fano factor of a stochastic sequestration feedback system in the limit of infinitely large sequestration affinity.

Here we describe the first moment model of the sequestration feedback system with two plant species and no controller degradation:

$$\begin{aligned}
\frac{d}{dt}\mathbb{E}[X_1] &= \theta_1\mathbb{E}[Z_1] - \gamma\mathbb{E}[X_1] \\
\frac{d}{dt}\mathbb{E}[X_2] &= k\mathbb{E}[X_1] - \gamma\mathbb{E}[X_2] \\
\frac{d}{dt}\mathbb{E}[Z_1] &= \mu - \eta\mathbb{E}[Z_1]\mathbb{E}[Z_2] - \eta\text{Cov}(Z_1, Z_2) \\
\frac{d}{dt}\mathbb{E}[Z_2] &= \theta_2\mathbb{E}[X_2] - \eta\mathbb{E}[Z_1]\mathbb{E}[Z_2] - \eta\text{Cov}(Z_1, Z_2).
\end{aligned}$$

Here θ_1 and k are the plant species production rates, γ is the plant species degradation rate, η is the strength of the sequestration reaction, and θ_2 is the rate of the plant output.

The stochastic sequestration feedback system's model is described and analyzed in the supplement, Section 6.8. The derivation for the Fano factor requires moment closure, which holds for an approximate model when η is large and when Z_2 is close to zero. Then the sequestration feedback system has Fano factor

$$\text{Fano}[X_2] = \frac{\text{Var}[X_2]}{\mathbb{E}[X_2]} = \frac{\gamma(2\theta_1 k + k\gamma + 2\gamma^2)}{2\gamma^3 - \theta_1\theta_2 k} \tag{12}$$

Simultaneously, the stability criterion for the deterministic sequestration feedback system with no controller degradation is

$$\gamma > \sqrt[3]{\frac{\theta_1\theta_2 k}{2}}, \tag{13}$$

as obtained by applying the production-degradation inequality in Section 2.2.

We infer from Equations (12) and (13) that the denominator of the Fano factor expression $2\gamma^3 - \theta_1\theta_2 k$ approaches 0 when $\gamma = \sqrt[3]{\frac{\theta_1\theta_2 k}{2}}$, which is the critical point at which the deterministic sequestration feedback system crosses from stability to instability.

Furthermore, the variance of the stochastic sequestration feedback system increases as the deterministic sequestration feedback system approaches the critical stability point, which corresponds to increasingly larger oscillations. Moreoever, the deterministic sequestration feedback system exhibits a tradeoff between response speed and instability (oscillations), while the stochastic sequestration feedback system has a tradeoff between the response speed of the mean and the variance. Thus, there is an intimate connection between the sensitivity of the deterministic sequestration feedback system, which appears as oscillatory behavior, and the sensitivity of the stochastic sequestration feedback system, which appears as an increase in the variance.

5 Conclusion

Feedback is an integral aspect of biological circuits, capturing the basic notion of sensing and decision making we often study in living systems. This works laid out an in-depth theoretical exploration of a particular feedback mechanism involving the sequestration reaction, which is both general enough to be implemented in a variety of biological contexts and sophisticated enough to yield many of the interesting tradeoffs intrinsic to engineering control systems. We showed that it is possible to gain an precise understanding of the relationships between speed, steady-state error, variability, and robustness through a variety of theoretical tools borrowed from classical control theory.

The broader scope of this work is to motivate further exploration of the mathematical structure of biological circuits. While our results yield insight into a particular model of biomolecular control, it is

an open question how many of our results are intrinsic to *any* biological control system and what is particular to the sequestration model. Further, our model assumes that all reactions in the plant are first order linear reactions. In the future, we plan to explore how the many nonlinearities often found in natural system (e.g., cooperativity, saturation) affect the qualitative nature of our results.

From an experimental perspective, we hope that our results will help guide both the analysis of natural biological circuits and the design of synthetic ones. While natural systems will undoubtedly be more complex than the ones studied here, we hope that our analysis will give a lens through which experimentalist can understand which properties of biomolecular feedback are the result of fundamental limitations on the system at hand and how tradeoffs can be an intrinsic aspect of circuit architecture.

6 Supplemental Information

6.1 Comparison of Linear and Nonlinear Model

Here we show simulations comparing the full nonlinear sequestration feedback system in Equation (1) as compared to the linearized system in Equation (3). We see in Figure 8 colored lines representing nonlinear simulations with black dashed lines showing the corresponding linearized trajectory. Generally, for stable and purely oscillatory regimes the two are indistinguishable.

The differences only becomes apparently when

$$\sqrt[n+1]{\frac{\theta_1\theta_2\prod_{i=1}^{n-1}k_i}{\Delta_n}} > \gamma$$

and the linear system has eigenvalues with positive real part. In this regime, the nonlinear model remains oscillatory and the linearized model will grow in an unbounded manner. In this sense, the nonlinear model is actually better behaved than its linearized counterpart. While the simulations here are only show a particular range of parameters, the results are consistent with all simulations we have attempted so far.

6.2 Stability Criterion

Here we consider a generalized sequestration feedback system with two control species (z_1 and z_2) and n plant species (x_1,...,x_n) with dynamics

$$\begin{aligned}
\dot{x}_1 &= \theta_1 z_1 - \gamma x_1 \\
\dot{x}_2 &= k_1 x_1 - \gamma x_2 \\
&\vdots \\
\dot{x}_n &= k_{n-1} x_{n-1} - \gamma x_n \\
\dot{z}_1 &= \mu - \eta z_1 z_2 \\
\dot{z}_2 &= \theta_2 x_2 - \eta z_1 z_2.
\end{aligned}$$

We can then describe the block structure of the linearized system in terms of the following matrices:

$$A = \begin{bmatrix} -\gamma & 0 & \cdots & 0 \\ k_1 & -\gamma & \cdots & 0 \\ 0 & \ddots & \ddots & \vdots \\ 0 & \cdots & k_{n-1} & -\gamma \end{bmatrix}, B = \begin{bmatrix} \theta_1 & 0 \\ \vdots & \vdots \\ 0 & 0 \end{bmatrix},$$

$$C = \begin{bmatrix} 0 & \cdots & 0 \\ 0 & \cdots & \theta_2 \end{bmatrix}, D = \begin{bmatrix} -\alpha & -\frac{\beta}{\alpha} \\ -\alpha & -\frac{\beta}{\alpha} \end{bmatrix},$$

$$M = \left[\begin{array}{c|c} A & B \\ \hline C & D \end{array}\right],$$

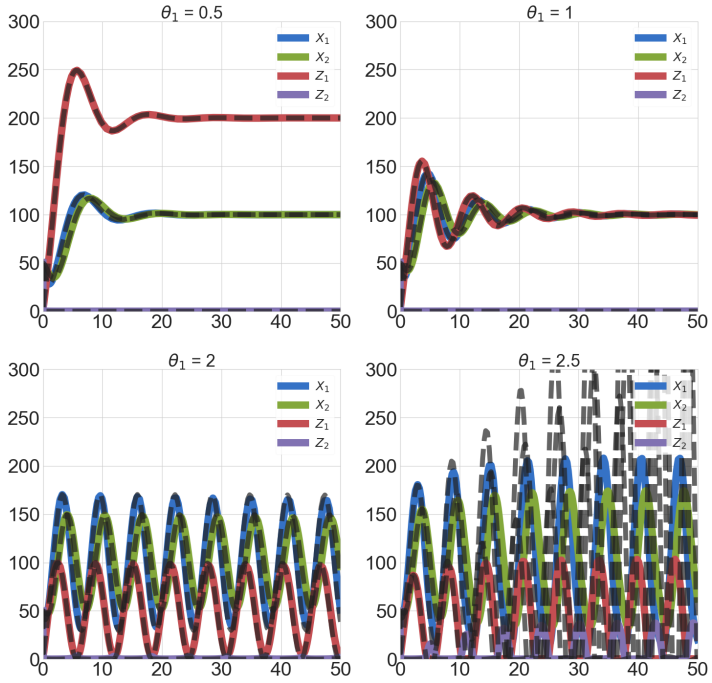

Figure 8: Comparison Of Nonlinear And Linearized Models. Here we see comparisons between nonlinear (colored lines) and linearized (dashed lines) trajectories for the sequestration feedback network with $n = 2$ plant species. The top two plots show two different stable trajectories, where linearization is indistinguishable from the original model. The bottom left plot shows oscillatory trajectories, where the linearized system has purely imaginary eigenvalues. This still shows a tight correspondence with the nonlinear system. The final plot shows the unstable regime of the linear system, where there are eigenvalues with positive real part. While the nonlinear system simply oscillates indefinitely, the linearized system grows unboundedly. For all simulations, $k = \theta_2 = \gamma = 1$, $\mu = 100$, $\eta = 100$, and θ_1 varies.

where $\alpha = \frac{\theta_1\theta_2\prod_{i=1}^{n-1} k_i}{\gamma^n}$ and $\beta = \eta\mu$. The linearized dynamics will then be of the form

$$\dot{\mathbf{v}} = M\mathbf{v},$$

where

$$\mathbf{v} = \begin{bmatrix} x_1 \\ \vdots \\ x_n \\ z_1 \\ z_2 \end{bmatrix}$$

To prove our main stability result, we will analyze the characteristic polynomial of M, $p(s)$. The roots of $p(s)$ correspond to eigenvalues of M. In general it is difficult to analyze these roots, however we will see that the $p(s)$ has a great deal of useful structure which we can exploit. First, we have to write down what $p(s)$ actually is.

Lemma 6.1. *The characteristic polynomial of M is*

$$p(s) = \det(sI - M) = (s+\gamma)^n[s^2 + (\alpha + \frac{\beta}{\alpha})s] + \gamma^n\beta.$$

Proof. We start by using the result that, for a block matrix such as M, we can use the classical result

from linear algebra

$$\begin{aligned} p(s) &= \det(sI - M) \\ &= \det\left[\begin{array}{c|c} sI - A & -B \\ \hline -C & sI - D \end{array}\right] \\ &= \det(sI - A)\det[(sI - D) - B(sI - A)^{-1}C]. \end{aligned}$$

Since A is lower-triangular, we see immediately that the first term is

$$\det(sI - A) = (s + \gamma)^n.$$

To analyze the second term, we first focus on computing $B(sI-A)^{-1}C$. Because of the sparse structure of B and C, we have

$$B(sI - A)^{-1}C = \begin{bmatrix} 0 & 0 \\ \theta_1\theta_2(sI - A)^{-1}_{n1} & 0 \end{bmatrix},$$

where $(sI - A)^{-1}_{n1}$ is the bottom-left most entry of $(sI - A)^{-1}$. Using Cramer's rule, we can compute

$$\begin{aligned} (sI - A)^{-1}_{n1} &= \frac{1}{(s+\gamma)^n}(-1)^{n+1}\det\begin{bmatrix} -k_1 & s+\gamma & \cdots & 0 \\ \vdots & \ddots & \ddots & \vdots \\ 0 & \cdots & -k_{n-2} & s+\gamma \\ 0 & 0 & \cdots & -k_{n-1} \end{bmatrix} \\ &= \frac{1}{(s+\gamma)^n}(-1)^{n+1}(-1)^{n-1}\prod_{i=1}^{n-1} k_i \\ &= \frac{\prod_{i=1}^{n-1} k_i}{(s+\gamma)^n}. \end{aligned}$$

Combing these results, we see that

$$\begin{aligned} p(s) &= (s+\gamma)^n \det\begin{bmatrix} s+\alpha & \frac{\beta}{\alpha} \\ \alpha - \frac{\theta_1\theta_2\prod_{i=1}^{n-1} k_i}{(s+\gamma)^n} & s + \frac{\beta}{\alpha} \end{bmatrix} \\ &= (s+\gamma)^n\left[(s+\alpha)(s+\frac{\beta}{\alpha}) - \beta + \frac{\gamma^n\beta}{(s+\gamma)^n}\right] \\ &= (s+\gamma)^n[s^2 + (\alpha + \frac{\beta}{\alpha})s] + \gamma^n\beta. \end{aligned} \tag{14}$$

□

we can now use this result about $p(s)$ to analyze the stability of the linearized sequestration feedback system.

Theorem 6.2 (Eigenvalue Classification Theorem)**.** *For a given n and $\beta \gg \alpha^2, \alpha\gamma$, the eigenvalues λ of M has a parameter-independent classification of the form $\left|\arg\left(\frac{\lambda}{\gamma}\right) + \arg\left(\frac{\lambda}{\gamma} + 1\right)\right| = m\pi$, for an integer m.*

Proof. To study the eigenvalues of M, we will analyze the roots of $p(s)$. We begin by by substituting $s = \gamma z$ in Equation (14) and setting $p(z) = 0$:

$$\gamma^2 z(1+z)^n\left[z + \frac{\alpha^2 + \beta}{\alpha\gamma}\right] = -\beta.$$

Taking the limit of strong feedback ($\beta \gg \alpha^2, \alpha\gamma$), this equation reduces to

$$z(1+z)^n\left[1 + z\frac{\alpha\gamma}{\beta}\right] = -\frac{\alpha}{\gamma}.$$

From this relationship we see that $p(z)$ has one large real root at $z \approx -\frac{\beta}{\alpha\gamma}$. If we plug this into the phase constraint equation, this gives a phase of $(n+1)\pi$. We will say the index of this root is $n+1$. If $|z| \ll \frac{\beta}{\alpha\gamma}$, we get the simplified magnitude constraint

$$|z||1+z|^n = \frac{\alpha}{\gamma}$$

and the phase constraint

$$\arg(z) + n\arg(1+z) = \pi + 2k\pi = (2k+1)\pi.$$

We can see from this that the maximum phase possible is $n+1$ and that any each of the indices will be of the form $2k+1$ (i.e., odd integers). Because the magnitude constraint is independent of k, fundamentally we can have phase indices for any odd integer m such that $|m| \leq n+1$.

First we will see what conditions can produce purely real roots. If z is real and $z > 0$, then

$$\arg(z) + n\arg(1+z) = 0,$$

which violates the phase constraint. This implies that, if there are unstable roots, they are not purely real. If $-1 < z < 0$, then

$$\arg(z) + n\arg(1+z) = \pi,$$

and we can have stable real roots with index 1. The magnitude constraint tells us that we will have a pair of these real roots if $\frac{\alpha}{\gamma} < \frac{n^n}{(n+1)^{n+1}}$ (which have index 1) with a bifurcation that generates conjugate pairs of roots when $\frac{\alpha}{\gamma} \geq \frac{n^n}{(n+1)^{n+1}}$. These conjugate roots will have indices ± 1.

An immediate result of these observations is that, for any positive odd integer m such that $1 < m < n+1$, roots cannot be purely real and must come in conjugate pairs $\pm m$. If n is odd, then we will have a conjugate pair of roots for each $m \in [3, n-1]$, either a pair of small real roots or a conjugate pair for $m = 1$, and a single large negative real root for $m = n+1$.

If n is odd, then the situation will be almost the same except for the fact that there will be a second real root with index $n+1$. By some simple accounting, this analysis accounts for all $n+1$ roots of $p(z)$, which correspond to roots of $p(s)$ by a simple rescaling by $\frac{1}{\gamma}$. □

Theorem 6.3 (Production-Degradation Inequality)**.** *Let M be the matrix corresponding to a linearization of the sequestration feedback system with two control molecules (z_1 and z_2) and n plant species. In the limit of strong feedback ($\beta \gg \alpha^2, \alpha\gamma$), the system is stable if and only if $\sqrt[n+1]{\frac{\theta_1\theta_2\prod_{i=1}^{n-1}k_i}{\Delta_n}} < \gamma$, where Δ_n is a constant that only depends on n. Further, when the system has purely imaginary eigenvalues the frequency of oscillation will be $\omega = \tan(\frac{\pi}{2n})\gamma$.*

Proof. We will prove the results by finding parametric conditions that will result in purely imaginary eigenvalues, and then study what happens to the stability of the system when those parametric conditions do not hold (i.e. equalities become inequalities). To do this, we generalize a technique from [4], where we evaluate $p(s) = 0$ on the imaginary axis. In particular, we pick the change of variable $s = i\delta\gamma$, where δ is a positive real number (which we can assume without loss of generality because complex roots come in conjugate pairs), and evaluate $p(\delta)$. This yields the equations

$$p(\delta) = 0 \implies \gamma^2 i\delta(1+i\delta)^n(\rho + i\delta) = -\beta, \tag{15}$$

where $\rho = \frac{\alpha^2+\beta}{\alpha\gamma}$. If we take the magnitude and phase of the the left-hand side of Equation (15), we get the constraints

$$\gamma^2\delta(1+\delta^2)^{\frac{n}{2}}\sqrt{\rho^2+\delta^2} = \beta \tag{16}$$

$$n\tan^{-1}(\delta) + \tan^{-1}\left(\frac{\delta}{\rho}\right) = \frac{\pi}{2} + 2k\pi. \tag{17}$$

From Theorem 6.2 we know that, in the limit of strong feedback, all complex eigenvalues have magnitude much less than ρ, therefore $\tan^{-1}(\delta/\rho) \to 0$. From these observations, we get the simplified relationship

$$n\tan^{-1}(\delta) = \frac{\pi}{2} + 2k\pi \implies \delta = \tan\left(\frac{\pi}{2n} + \frac{2k}{n}\pi\right).$$

and Equation (16) becomes

$$\delta(1+\delta^2)^{\frac{n}{2}}\frac{\gamma}{\alpha}=1$$

$$\implies \gamma=\sqrt[n+1]{\frac{\theta_1\theta_2\prod_{i=1}^{n-1}k_i}{\Delta_n}}, \tag{18}$$

where $\Delta_n=\delta(1+\delta^2)^{\frac{n}{2}}$. We can think of the parametric constrain Equation (18) as the boundary between stable and unstable behavior in the system. Because the left-hand side of Equation (16) is monotone in δ, we can infer that δ is unique and consequently there can only be one point in parameter space where there exist purely imaginary eigenvalues.

The final step is to study what happens when Equation (18) does not hold. First we look at the regime $\sqrt[n+1]{\frac{\theta_1\theta_2\prod_{i=1}^{n-1}k_i}{\Delta_n}}<\gamma$. Again using the uniqueness of δ, if we understand the stability behavior of the system for a particular value of γ in this regime, the same stability behavior must hold for all γ in this range. Because of this, we can first examine the range where γ is large. Intuitively, if degradation is sufficiently stronger than production then all species subject to degradation should converge to 0. To prove this rigorously, we will first search for roots with a large magnitude. If we apply the strong feedback limit to the characteristic equation from Equation (14), we get

$$p(s)=s(s+\gamma)^n(s+\frac{\beta}{\alpha})+\gamma^n\beta=0$$

$$\implies s\left(\frac{s}{\gamma}+1\right)^n\left(s\frac{\gamma\alpha}{\beta}+1\right)+\gamma\alpha=0.$$

When $|s|\gg\gamma\alpha$, the characteristic equation will have the approximate form

$$\left(\frac{s}{\gamma}+1\right)^n\left(s\frac{\gamma\alpha}{\beta}+1\right)=0,$$

which gives us n roots at $-\gamma$ and one root at $-\frac{\beta}{\gamma\alpha}$. Since Equation (14) is order $n+2$, we know there is one remaining root outside of this regime. Next, we search for the final small root ($|s|\ll\min(\gamma,\frac{\beta}{\gamma\alpha})$, which gives relationship

$$s+\gamma\alpha=0,$$

which gives a final small root at $-\gamma\alpha$. Since each of the $n+2$ roots is negative, the system is stable for all $\sqrt[n+1]{\frac{\theta_1\theta_2\prod_{i=1}^{n-1}k_i}{\Delta_n}}<\gamma$.

Now we examine the regime $\sqrt[n+1]{\frac{\theta_1\theta_2\prod_{i=1}^{n-1}k_i}{\Delta_n}}>\gamma$. Here we will use a different technique, as taking the analogous limit of very small γ is less straight-forward to analyze. To start, we will perform a change of variable $s=\gamma z$, where $z\in\mathbb{C}$. We will again using the strong feedback limit, and study roots near the stability boundary, such that the characteristic equation still has the general form

$$z(1+z)^n=-\frac{\alpha}{\gamma}.$$

If we write $z=a+ib$, we have the magnitude constraint

$$(a^2+b^2)[(1+a)^2+b^2]^n=\left(\frac{\alpha}{\gamma}\right)^2>\Delta_n^2.$$

We also get the phase relationship

$$\tan^{-1}(\frac{b}{a})+n\tan^{-1}(\frac{b}{1+a})=\pi$$

$$\implies \frac{b}{1+a}<\delta.$$

Combining these relationships, we get

$$[a^2 + \delta^2(1+a)^2](1+\delta^2)^n(1+a)^{2n} > \Delta_n^2.$$
$$\implies \left[\left(\frac{a}{\delta}\right)^2 + (1+a)^2\right](1+a)^{2n} > 1.$$

Since $a = 0$ at the stability boundary, there must be a regime of parameters sufficiently close to the boundary such that $|a| \ll \delta$, for which we have the relationship

$$(1+a)^{2(n+1)} > 1 \implies a > 0.$$

This proves the existence of an unstable point when $\sqrt[n+1]{\frac{\theta_1\theta_2\prod_{i=1}^{n-1}k_i}{\Delta_n}} > \gamma$, which implies that all parameters in this regime will yield unstable dynamics (so long as the strong feedback assumption still holds). □

We note that, thought previous results studied the regime of strong feedback (β large), the core assumption that was made is that the quantity

$$\frac{\alpha^2+\beta}{\alpha\gamma} \gg 1.$$

We note that there is an entirely different way to achieve this, by making $\alpha^2 \gg \beta, \alpha\gamma$. In this regime, all of the previous results follow in almost exactly the same way, except for changes to the constants involved. It is relatively straightforward to show that the characteristic equation for the system reduces to

$$z(1+z)^n = -\frac{\beta\gamma}{\alpha}.$$

Following the same steps from the previous proofs, we can find that instability now occurs when

$$\sqrt[n-1]{\frac{\Delta_n\theta_1\theta_2\prod_{i=1}^{n-1}k_i}{\beta}} = \gamma.$$

Interestingly, the stable regime is now

$$\sqrt[n-1]{\frac{\Delta_n\theta_1\theta_2\prod_{i=1}^{n-1}k_i}{\beta}} > \gamma,$$

the opposite of what occurs in the strong feedback limit. One interpretation of these results as a whole is that stability is achievable when either controller sequestration or plant degradation are individually large, but not when both are large simultaneously.

6.3 The Sensitivity Function

The sensitivity function $S(s), s \in \mathbb{C}$ is the transfer function between the output of a system and disturbances to its state [2]. It is particularly useful to examine $|S(i\omega)|$, which corresponds to the magnitude of S given a purely oscillatory disturbance. If $|S(i\omega)| > 1$, then the system will amplify disturbances at a frequency ω. Conversely, if $|S(i\omega)| < 1$ then the system will attenuate disturbances at frequency ω.

Define $P(s)$ and $C(s)$ to be the transfer function between inputs and outputs of the plant and controller, respectively. It is a standard result in control theory that

$$S = \frac{1}{1+PC}.$$

In general, for a linear system

$$\begin{aligned} \dot{x} &= Ax + Bu \\ y &= Cx, \end{aligned}$$

the transfer function has the form $H(s) = C(sI - A)^{-1}B$. For the sequestration feedback system, we have that

$$P(s) = [0, \cdots, 1](sI - A)^{-1} \begin{bmatrix} 0 \\ \vdots \\ \theta_1 \end{bmatrix} = \frac{\theta_1 \prod_{i=1}^{n-1} k_i}{(s+\gamma)^n},$$

where just as before we use

$$A = \begin{bmatrix} -\gamma & 0 & \cdots & 0 \\ k_1 & -\gamma & \cdots & 0 \\ 0 & \ddots & \ddots & \vdots \\ 0 & \cdots & k_{n-1} & -\gamma \end{bmatrix}.$$

Similarly, we have that

$$C(s) = [0, -1](sI - D)^{-1} \begin{bmatrix} 0 \\ \theta_2 \end{bmatrix} = \frac{1}{s} \frac{\theta_2 \frac{\beta}{\alpha}}{[s + (\alpha + \frac{\beta}{\alpha})]},$$

where

$$D = \begin{bmatrix} -\alpha & -\frac{\beta}{\alpha} \\ -\alpha & -\frac{\beta}{\alpha} \end{bmatrix}.$$

Here, the output has the form $[0, -1]$ because in the standard formulation of these results it is assumed that the output of the controller (z_1 in our case) is used for negative feedback. Since z_1 has a positive sign in $\dot{x}_1$, we flip the sign to be consistent. Note that $C(s)$ has a factor if $\frac{1}{s}$, indicating that it corresponds to an integrator. From P and C, we see that

$$S = \frac{1}{1 + \frac{\frac{\beta}{\alpha}\theta_1\theta_2 \prod_{i=1} n-1 k_i}{s(s+\gamma)^n[s+(\alpha+\frac{\beta}{\alpha})]}} = \frac{s(s+\gamma)^n[s + (\alpha + \frac{\beta}{\alpha})]}{s(s+\gamma)^n[s + (\alpha + \frac{\beta}{\alpha})] + \beta\gamma^n}.$$

If we again take the limit $\frac{\alpha+\frac{\beta}{\alpha}}{\gamma} \gg 1$ and substitute $s = \gamma z$ we get the approximation

$$S(z) \approx \frac{z(1+z)^n}{z(1+z)^n - \frac{\alpha}{\gamma}}.$$

Ideally we would like to analyze $\|S(i\omega)\|_\infty = \max_\omega |S(i\omega)|$, however this is difficult to compute in general. A lower bound for this term can, however, be easily computed by evaluating a particular value of ω close to the maximum. Specifically, we will use $\omega = \tan(\frac{\pi}{2n})\gamma = \delta\gamma$. At $z = i\delta$, we get

$$|S(i\delta)| \approx \frac{\delta(1+\delta^2)^{\frac{n}{2}}}{\delta(1+\delta^2)^{\frac{n}{2}} - \frac{\alpha}{\gamma}} = \frac{\Delta_n}{\Delta_n - \frac{\alpha}{\gamma}}.$$

From our previous results, we know that the system is purely oscillatory when $\Delta_n = \frac{\alpha}{\gamma}$, which corresponds to $|S(i\delta)| = \|S(i\omega)\|_\infty = \infty$. This gives the intuitive result that the system is infinitely sensitive to a periodic disturbance at $\omega = \delta\gamma$ when $\Delta_n = \frac{\alpha}{\gamma}$. In general, we will have that

$$\|S(i\omega)\|_\infty \geq \frac{\Delta_n}{\Delta_n - \frac{\alpha}{\gamma}}.$$

6.4 Incorporating the Controller Species Degradation Into the Model

6.4.1 Integral Controller

Without the degradation of the controller species in the model description, Equations (1c), (1d) describe the controller species as:

$$\begin{aligned} \dot{z}_1 &= \mu - \eta z_1 z_2, \\ \dot{z}_2 &= \theta x_2 - \eta z_1 z_2. \end{aligned} \tag{19}$$

We define the error signal as $e(t) = \frac{\mu}{\theta} - x_n(t)$.
The controller species implement integral control since

$$\frac{d}{dt}(z_1(t) - z_2(t)) = \theta\Big(\frac{\mu}{\theta} - x_n(t)\Big). \tag{20}$$

The control action $z_1(t) - z_2(t)$ integrates the error signal $e(t)$

$$z_1(t) - z_2(t) = \theta \int_0^t (e(s))\, ds. \tag{21}$$

If a steady state of the model exists, then the integral controller has the property that the steady state error is zero since:

$$\frac{dz_1(t)}{dt} = \frac{dz_2(t)}{dt} = 0 \implies x_n^{ss} = \frac{\mu}{\theta} \tag{22}$$

Achieving zero steady state error is a desirable property for the sequestration feedback system because it does not directly depend on the dynamics of the plant. We investigate whether this property is retained by including the controller species degradation in the model.

6.4.2 Lag Compensator

Incorporating the degradation of the controller species in the model description changes the controller Equations (19) to the following:

$$\begin{aligned} \dot{z}_1 &= \mu - \eta z_1 z_2 - \gamma_c z_1, \\ \dot{z}_2 &= \theta x_2 - \eta z_1 z_2 - \gamma_c z_2. \end{aligned} \tag{23}$$

The resulting controller is a lag compensator that integrates the error signal weighed by an exponential of the controller degradation rate:

$$\frac{d}{dt}(z_1(t) - z_2(t)) = \mu - \theta x_n(t) - \alpha(z_1(t) - z_2(t)), \tag{24}$$

$$z_1(t) - z_2(t) = \theta \int_0^t e^{\alpha(s-t)} \left(\frac{\mu}{\theta} - x_n(t)\right) ds. \tag{25}$$

The exponential of the degradation rate biases the error measurement towards recent past over the distant past.

Integral control has the property of perfect adaptation, provided that the closed loop system in stable. This means that the closed loop system has zero steady state error. The lag compensator can also exhibit perfect adaptation at a critical controller degradation rate.

6.5 The critical controller species degradation rate

We derive the critical controller species degradation rate γ_c such that the steady state error of a general sequestration feedback network with n plant species equals zero. We also derive conditions such that the critical controller degradation rate is achievable by the network parameters and we demonstrate that it is unique.

We consider the general deterministic sequestration feedback network with n plant species (i.e. the n plant species can be reactants in any bimolecular reactions within the plant network). Then the

model of its dynamics is given by:

$$\begin{aligned}
\frac{dx_1}{dt} &= \theta_1 z_1 + \alpha_{1,1}x_1 + \cdots + \alpha_{1,n}x_n,\\
\frac{dx_2}{dt} &= \alpha_{2,1}x_1 + \cdots + \alpha_{2,n}x_n,\\
&\vdots\\
\frac{dx_n}{dt} &= \alpha_{n,1}x_1 + \cdots + \alpha_{n,n}x_n,\\
\frac{dz_1}{dt} &= \mu - \eta z_1 z_2 - \gamma_c z_1,\\
\frac{dz_2}{dt} &= \theta_2 x_n - \eta z_1 z_2 - \gamma_c z_2.
\end{aligned} \tag{26}$$

We define the following notation:

$$A = \begin{pmatrix} \alpha_{2,1} & \alpha_{2,2} & \dots & \alpha_{2,n-1} \\ \vdots & \vdots & \vdots & \vdots \\ \alpha_{n,1} & \alpha_{n,2} & \dots & \alpha_{n,n-1} \end{pmatrix},$$

$\alpha_1 = (\alpha_{1,1}, \dots, \alpha_{1,n-1})$, $\alpha_n = (\alpha_{2,n}, \dots, \alpha_{n,n})^T$, and $\Gamma = \theta_1^{-1}(\alpha_1 A^{-1}\alpha_n - \alpha_{1,n})$.

Theorem 6.4. *The critical controller degradation rate of a general sequestration feedback network with n plant species is given by*

$$\gamma_c = \frac{\theta_2}{\Gamma} - \frac{\Gamma\eta\mu}{\theta_2} \tag{27}$$

and it only exists if and only if the closed loop system has a steady state and $\Gamma < \frac{\theta_2}{\sqrt{\eta\mu}}$

Proof. In a 1-node sequestration feedback system, the degradation rate

$$\gamma_c = \frac{\theta_1\theta_2}{\gamma_p} - \frac{\gamma_p\eta\mu}{\theta_1\theta_2}$$

results in zero steady state error. This degradation rate value can only be achieved when $\gamma_p < \frac{\theta_1\theta_2}{\sqrt{\mu\eta}}$.

Assuming that a steady state exists, then Equation (26) reduces to

$$\begin{aligned}
0 &= \theta_1 z_1 + \alpha_{1,1}x_1 + \cdots + \alpha_{1,n}x_n\\
0 &= \alpha_{2,1}x_1 + \cdots + \alpha_{2,n}x_n\\
&\vdots\\
0 &= \alpha_{n,1}x_1 + \cdots + \alpha_{n,n}x_n\\
\mu &= \eta z_1 z_2 + \gamma_c z_1,\\
\theta_2 x_n &= \eta z_1 z_2 + \gamma_c z_2.
\end{aligned} \tag{28}$$

Our system of equations in (28) reduces to

$$\begin{aligned}
z_1 &= \Gamma x_n,\\
\mu &= \eta z_1 z_2 + \gamma_c z_1,\\
\theta x_n &= \eta z_1 z_2 + \gamma_c z_2.
\end{aligned} \tag{29}$$

First it must be the case that constant $\Gamma > 0$ and matrix A is invertible. Otherwise, the system cannot have a positive steady state. This is equivalent to $\alpha_1 A^{-1}\alpha_n > \alpha_{1,n}$. The input species should not be depleted to create the output species. The system in Equation (29) simplifies to a single equation

$$x_n^2(\Gamma\eta\theta_2 + \Gamma^2\eta\gamma_c) + x_n(\Gamma\gamma_c^2 - \Gamma\mu\eta) - \gamma_c\mu = 0. \tag{30}$$

Equation (30) always has a positive solution

$$x_n = \frac{(\Gamma\mu\eta - \Gamma\gamma_c^2) + \sqrt{(\Gamma\gamma_c^2 - \Gamma\mu\eta)^2 + 4\gamma_c\mu(\Gamma\eta\theta_2 + \Gamma^2\gamma_c\eta)}}{2(\Gamma\eta\theta_2 + \Gamma^2\gamma_c\eta)}. \tag{31}$$

Thus, the steady state error signal is

$$e = \frac{-(\Gamma\gamma_c^2 + 2\Gamma^2\gamma_c\frac{\eta\mu}{\theta_2} + \Gamma\mu\eta) + \sqrt{(\Gamma\gamma_c^2 - \Gamma\mu\eta)^2 + 4\gamma_c\mu(\Gamma\eta\theta_2 + \Gamma^2\gamma_c\eta)}}{2(\Gamma^2\gamma_c\eta + \Gamma\eta\theta_2)}. \tag{32}$$

If we want the output of the dynamical system to follow the reference signal $\frac{\mu}{\theta_2}$, then it must be that

$$\gamma_c = \frac{\theta_2}{\Gamma} - \frac{\Gamma\eta\mu}{\theta_2}, \tag{33}$$

which can only be achieved if and only if $\Gamma < \frac{\theta_2}{\sqrt{\eta\mu}}$. □

Therefore, lag compensation can result in perfect adaptation for optimal values of the controller species degradation rate γ_c. Depending on the parameters of the sequestration feedback system, the optimal value of the degradation rate may or may not be achievable.

Remark 1. *If the n-species plant network has a cyclical structure (i.e. each plant species creates the next species and is degraded by the previous species), then the critical controller degradation rate is* $\gamma_c = \frac{\theta_1\theta_2\prod_{i=1}^{n-1}k_i}{\gamma_p^n} - \frac{\eta\mu\gamma_p^n}{\theta_1\theta_2\prod_{i=1}^{n-1}k_i}$.

In this particular case,

$$A^{-1} = \begin{pmatrix} \frac{1}{k_2} & \frac{\gamma_p}{k_2k_3} & \cdots & \frac{\gamma_p^{n-2}}{k_2\ldots k_{n-1}\theta_2} \\ 0 & \frac{1}{k_3} & \cdots & \frac{\gamma_p^{n-3}}{k_3\ldots k_{n-1}\theta_2} \\ \vdots & \vdots & \vdots & \vdots \\ 0 & 0 & \ldots & \frac{1}{\theta_2} \end{pmatrix},$$

$\beta_1 = (-\gamma_p, 0, \ldots, 0)$, $\beta_n = (0, \ldots, 0, -\gamma_p)^T$, $\beta_{1,n} = 0$, and $\Gamma = \frac{\gamma_p^n}{\prod_{i=1}^{n-1}k_i\theta_2}$. Hence

$$\gamma_c = \frac{\theta_1\theta_2\prod_{i=1}^{n-1}k_i}{\gamma_p^n} - \frac{\eta\mu\gamma_p^n}{\theta_1\theta_2\prod_{i=1}^{n-1}k_i}. \tag{34}$$

It can only be achieved if and only if

$$\gamma_p < \sqrt[n]{\frac{\theta_1\theta_2\prod_{i=1}^{n-1}k_i}{\sqrt{\eta\mu}}}. \tag{35}$$

6.6 Stability analysis of the sequestration feedback network with controller degradation

We derive criterion for the stability of the sequestration feedback system with controller degradation. The criterion changes according to the relationship between the plant degradation rate γ_p and the controller degradation rate γ_c.

We begin by denoting

$$\alpha = \frac{\theta_1\theta_2\prod_{i=1}^{n-1}k_i}{\gamma_p^n},$$

$$\beta = \eta\mu,$$

where γ_p is the degradation rate of the plant species and γ_c is the degradation in the controller species. The the matrix

$$D = \begin{bmatrix} -\alpha - \gamma_c & -\frac{\beta}{\alpha} \\ -\alpha & -\frac{\beta}{\alpha} - \gamma_c \end{bmatrix} \tag{36}$$

Therefore the characteristic polynomial is:

$$(s+\gamma_p)^n(s+\gamma_c)\left(s+\gamma_c+\frac{\beta}{\alpha}+\alpha\right)+\beta\gamma_p^n = 0 \tag{37}$$

We study the characteristic polynomial's roots to determine the stability of the closed loop system with controller species degradation.

First we make the change of variable $s = \gamma_p z$ and obtain a new formulation of the characteristic polynomial in Equation (37) as the following:

$$(z+1)^n\left(z+\frac{\gamma_c}{\gamma_p}\right)\left(z+\frac{\gamma_c+\alpha+\frac{\beta}{\alpha}}{\gamma_p}\right) = -\frac{\beta}{\gamma_p^2} \tag{38}$$

Let z be a complex root of the characteristic polynomial in Equation (38).

We use the characteristic polynomial in Equation (38) to derive the stability criterion for the sequestration feedback system. For simplicity, we make the strong feedback assumption. We consider the following three cases: $\gamma_c \ll \gamma_p$, γ_c and γ_p the same order of magnitude, and $\gamma_c \gg \gamma_p$.

Case I: $\gamma_c \ll \gamma_p$

In this case, the controller species degradation rate is much smaller than the plant species degradation rate and therefore it does not influence the stability of the closed loop sequestration feedback system.

In particular, the characteristic polynomial in Equation (38) reduces to the following characteristic polynomial:

$$z(z+1)^n\left(z+\frac{\alpha+\frac{\beta}{\alpha}}{\gamma_p}\right) = -\frac{\beta}{\gamma_p^2}. \tag{39}$$

We know from the supplement, Theorem 6.3 that the solution of the stability problem is provided by the production-degradation inequality. Therefore, in order for the closed loop sequestration feedback system to be stable, we must have that:

$$\gamma_p > \sqrt[n+1]{\frac{\theta_1\theta_2\prod_{i=1}^{n-1}k_i}{\Delta_n}}, \tag{40}$$
$$\gamma_p \gg \gamma_c.$$

Case II: γ_c, γ_p are the same order of magnitude

Then the characteristic polynomial is given by:

$$(z+1)^{n+1}\left(z+1+\frac{\alpha+\frac{\beta}{\alpha}}{\gamma_p}\right) = -\frac{\beta}{\gamma_p^2} \tag{41}$$

We assume that we are in the strong feedback limit of $\beta >> \alpha^2, \alpha\gamma_p$. We multiply both side of the characteristic polynomial by factor $\frac{\gamma_p\alpha}{\beta}$.

Hence we obtain that

$$(z+1)^{n+1}\left(z\frac{\gamma_p\alpha}{\beta}+\frac{\gamma_p\alpha}{\beta}+\frac{\alpha^2}{\beta}+1\right) = -\frac{\alpha}{\gamma_p}, \tag{42}$$

which, under the strong feedback assumption, simplifies to

$$(z+1)^{n+1}\left(z\frac{\gamma_p\alpha}{\beta}+1\right)=-\frac{\alpha}{\gamma_p}, \tag{43}$$

Therefore, the largest real root is at value $\approx -1-\frac{\beta}{\gamma_p\alpha}$.

If n is even, then the characteristic polynomial in (43) has two negative real roots and the remaining roots are conjugate complex pairs.

To determine the stability criterion, we analyze the bifurcation point at which the system goes from stable to unstable. Therefore, we assume that there is a complex root $z=i\delta$. Then the magnitude and phase of the characteristic polynomial are given by

$$\begin{aligned}(\delta^2+1)^{\frac{n+1}{2}}&=\frac{\alpha}{\gamma_p},\\ \tan^{-1}(\delta)&=\frac{\pi(2k+1)}{n+1},\end{aligned} \tag{44}$$

where $0\le k\le\frac{n}{2}$.

The second real root corresponds to index $k=\frac{n}{2}$.

We follow the proof in Theorem 6.3 and we obtain that stability is guaranteed if

$$\begin{aligned}&\text{n is even},\\ &\gamma_c\approx\gamma_p,\\ &\gamma_p>\frac{\sqrt[n+1]{\theta_1\theta_2\prod_{i=1}^{n-1}k_i}}{\sqrt{\tan(\frac{\pi}{n+1})^2+1}}.\end{aligned} \tag{45}$$

If n is odd, then the characteristic polynomial in (43) has only one negative real root, located at value $\approx -1-\frac{\alpha+\frac{\beta}{\alpha}}{\gamma_p}$. The other roots are conjugate complex pairs. The rest of the argument is similar and stability is guaranteed for an analogous criterion.

Case III: $\gamma_c\gg\gamma_p$

We can equivalently write the characteristic polynomial in Equation (38) as the following:

$$(z+1)^n\left(z\frac{\gamma_p}{\gamma_c}+1\right)\left(z\frac{\alpha\gamma_p}{\alpha\gamma_c+\beta}+1\right)=-\frac{\alpha}{\gamma_c} \tag{46}$$

Since $\frac{\gamma_p}{\gamma_c}$ and $\frac{\alpha\gamma_p}{\alpha\gamma_c+1}$ are very small, we can infer that the characteristic polynomial (46) has two large negative real roots at values $\approx-\frac{\gamma_c}{\gamma_p}$ and $\approx-\frac{\gamma_c}{\gamma_p}-\frac{\beta}{\alpha\gamma_p}$. Here we have assumed that $\beta\gg\alpha\gamma_c$ in addition to the strong feedback assumption.

We only consider the case n even. The case n odd has a similar proof with an additional real root.

Then the magnitude and the phase of the characteristic polynomial are given by:

$$\begin{aligned}(\delta^2+1)^{\frac{n}{2}}&=\frac{\alpha}{\gamma_c},\\ \tan^{-1}(\delta)&=\frac{\pi(2k+1)}{n},\end{aligned} \tag{47}$$

where $0\le k\le\frac{n}{2}-1$.

All the roots are conjugate complex and they occur in pairs.

If the following conditions

$$\begin{aligned}&\gamma_c\gg\gamma_p,\\ &\gamma_p>\frac{\sqrt[n]{\theta_1\theta_2\prod_{i=1}^{n-1}k_i}}{\sqrt[n]{\gamma_c}\sqrt{1+\tan\left(\frac{\pi}{n}\right)^2}},\end{aligned} \tag{48}$$

hold, then the stability of the closed loop sequestration feedback system is guaranteed.

6.7 Stability of the sequestration feedback system with two plant species and controller species degradation

For this simple sequestration feedback system with two plant species and two controller species subjected to degradation, we derive the stability criterion for general values of the plant degradation rate γ_p and the controller degradation rate γ_c.

Here we compute the matrix

$$D = \begin{bmatrix} -\eta_2 - \gamma_c & -\eta_1 \\ -\eta_2 & -\eta_1 - \gamma_c \end{bmatrix}, \tag{49}$$

where

$$\eta_1 = \eta\mu \frac{\gamma_p^n}{\theta_1\theta_2 \prod_{i=1}^{n-1} k_i}$$

$$\eta_2 = \frac{\theta_1\theta_2 \prod_{i=1}^{n-1} k_i}{\gamma_p^n}.$$

The characteristic polynomial is:

$$(\gamma_p + s)^n(\gamma_c + s)(\eta_1 + \eta_2 + \gamma_c + s) + \eta_1\theta_1\theta_2 \prod_{i=1}^{n-1} k_i = 0 \tag{50}$$

Assume $\mu\eta$ is large, then:

$$(\gamma_p + s)^n(\gamma_c + s) + \theta_1\theta_2 \prod_{i=1}^{n-1} k_i = 0 \tag{51}$$

Let $s = wi$. Then,

$$(\gamma_p + wi)^n(\gamma_c + wi) + \theta_1\theta_2 \prod_{i=1}^{n-1} k_i = 0 \tag{52}$$

Consider the magnitude of the equation:

$$(\gamma_p^2 + w^2)^n(\gamma_c^2 + w^2)^2 = (\theta_1\theta_2 \prod_{i=1}^{n-1} k_i)^2 \tag{53}$$

and the phase of the equation:

$$\tan^{-1}\frac{w}{\gamma_c} + n\tan^{-1}\frac{w}{\gamma_p} = \pi \tag{54}$$

If $n = 2$, when the imaginary component of (52) is set to 0, we can solve for $w = \sqrt{(2\gamma_c + \gamma_p)\gamma_p}$. Then,

$$(\gamma_p^2 + w^2)(\gamma_c^2 + w^2) = \theta_1\theta_2 k \tag{55}$$

$$\gamma_p(\gamma_c + \gamma_p)^2 = \frac{\theta_1\theta_2 k}{2} \tag{56}$$

The stability criteria is (by Descartes' rule of sign)

$$\gamma_p(\gamma_c + \gamma_p)^2 \geq \frac{\theta_1\theta_2 k}{2} \tag{57}$$

6.8 Stochastic analysis

We derive the Fano factor of a stochastic sequestration feedback system with two plant species. We describe the biochemical reactions of sequestration feedback system with two plant species:

$$\emptyset \xrightarrow{\mu} Z_1 \qquad Z_1 \xrightarrow{\theta_1} Z_1 + X_1 \qquad X_1 \xrightarrow{k} X_2 \qquad X_2 \xrightarrow{\theta_2} X_2 + Z_2$$
$$X_1 \xrightarrow{\gamma} \emptyset \qquad X_2 \xrightarrow{\gamma} \emptyset$$
$$Z_1 + Z_2 \xrightarrow{\eta} \emptyset.$$

If we assume infinitely strong binding of the sequestration reaction, then limit $\eta \to \infty$ holds. Hence, at any time, only one of species Z_1 and Z_2 can be non-zero. If both species are non-zero, then they sequestrate each other infinitely fast through reaction $Z_1 + Z_2 \to \emptyset$ until one of them become zero. Therefore, we can define variable $Z = Z_1 - Z_2$, which has a one-to-one correspondence to species Z_1 and Z_2 counts, where positive Z indicates counts of Z_1, and negative Z indicates counts of Z_2.

With this simplification, the dynamics of the stochastic sequestration feedback system can be described by a continuous-time Markov chain (CTMC) over the counts of species Z, X_1 and X_2 using the following master equation dynamics [7]:

$$\begin{aligned}\dot{p}(x_1, x_2, z) = \mu(p(x_1, x_2, z-1) - p(x_1, x_2, z)) \\ + \theta_1 \max\{z, 0\}[p(x_1 - 1, x_2, z) - p(x_1, x_2, z)] \\ + k x_1 [p(x_1, x_2 - 1, z) - p(x_1, x_2, z)] \\ + \theta_2 x_2 [p(x_1, x_2, z+1) - p(x_1, x_2, z)] \\ + \gamma[(x_1+1)p(x_1+1, x_2, z) - x_1 p(x_1, x_2, z)] \\ + \gamma[(x_2+1)p(x_1, x_2+1, z) - x_2 p(x_1, x_2, z)],\end{aligned} \tag{58}$$

where $p(x_1, x_2, z; t)$ denotes the probability for the system to have $Z = z$, $X_1 = x_1$, and $X_2 = x_2$ at time t.

We observe that all the terms on the right hand side of Equation (58) are linear, except for the $\max\{z, 0\}$ term. We can see this more clearly if we consider the first moment equation.

If we consider the steady-state master equation, we set the left hand side to 0 and we apply $\sum_{x_1, x_2, z} x_1$ with the sum over all $x_1, x_2 \in \mathbb{N}, z \in \mathbb{Z}$, then we obtain that

$$\theta_1 \mathbb{E}(Z | Z \geq 0) \mathbb{P}(Z \geq 0) = \gamma \mathbb{E} X_1 \tag{59}$$

Similarly, if we apply $\sum_{x_1, x_2, z} x_2$, and $\sum_{x_1, x_2, z} z$, we get

$$k \mathbb{E} X_1 = \gamma \mathbb{E} X_2 \qquad \mu = \theta_2 \mathbb{E} X_2. \tag{60}$$

The term that prevents us from solving this set of linear equations for the first moments is the $\max\{z, 0\}$ term, which results in the probability for Z to be non-negative in the moment equations.

Therefore, we make a second assumption that $Z \geq 0$ with probability 1 at steady state. This means Z_2 is zero with probability 1 and this represents a good approximation if the system is stable, without Z_1 oscillating to a very low count.

Under this assumption, we then obtain that

$$\theta_1 \mathbb{E} Z = \gamma \mathbb{E} X_1, \tag{61}$$

which is a linear equation.

Similarly, if we apply sum $\sum_{x_1, x_2, z} x_1 z$ to the master equation, we obtain a system of linear equations for steady-state moments of both the first and the second order terms. Solving this system of equations then gives the following result for the Fano factor:

$$\frac{\operatorname{Var} X_2}{\mathbb{E} X_2} = \frac{\gamma(2\theta_1 k + k\gamma + 2\gamma^2)}{2\gamma^3 - \theta_1 \theta_2 k} \tag{62}$$

As $\gamma \to \infty$, we obtain an additional simplification

$$\frac{\text{Var}\, X_2}{\mathbb{E}X_2} \sim 1 + \frac{k}{2\gamma} \tag{63}$$

We also derive the Fano factor for the three plant species stochastic sequestration feedback system and we obtain an analogous result,

$$\frac{\text{Var}\, X_3}{\mathbb{E}X_3} = \frac{8\gamma^4 + 3k_2\gamma^3 + 3k_1k_2\gamma^2 + 8\theta_1k_1k_2\gamma - 3\theta_1\theta_2k_1k_2}{8\gamma^4 - 9\theta_1\theta_2k_1k_2}. \tag{64}$$

The denominator in Equation (64) matches the stability criterion for the three plant species deterministic sequestration feedback system.

References

[1] Ang, J., Bagh, S., Ingalls, B. P., and McMillen, D. R. (2010). Considerations for using integral feedback control to construct a perfectly adapting synthetic gene network. *Journal of theoretical biology*, 266(4):723–738.

[2] Aström, K. J. and Murray, R. M. (2010). *Feedback systems: an introduction for scientists and engineers*. Princeton university press.

[3] Bernstein, J. A., Lin, P.-H., Cohen, S. N., and Lin-Chao, S. (2004). Global analysis of escherichia coli rna degradosome function using dna microarrays. *Proceedings of the National Academy of Sciences of the United States of America*, 101(9):2758–2763.

[4] Briat, C., Gupta, A., and Khammash, M. (2016). Antithetic integral feedback ensures robust perfect adaptation in noisy biomolecular networks. *Cell Systems*, 2(1):15 – 26.

[5] Chandra, F. A., Buzi, G., and Doyle, J. C. (2011). Glycolytic oscillations and limits on robust efficiency. *science*, 333(6039):187–192.

[6] De Jonge, N., Garcia-Pino, A., Buts, L., Haesaerts, S., Charlier, D., Zangger, K., Wyns, L., De Greve, H., and Loris, R. (2009). Rejuvenation of ccdb-poisoned gyrase by an intrinsically disordered protein domain. *Molecular cell*, 35(2):154–163.

[7] Del Vecchio, D. and Murray, R. M. (2015). *Biomolecular feedback systems*. Princeton University Press.

[8] El-Samad, H., Kurata, H., Doyle, J., Gross, C., and Khammash, M. (2005). Surviving heat shock: control strategies for robustness and performance. *Proceedings of the National Academy of Sciences of the United States of America*, 102(8):2736–2741.

[9] Gallego, M. and Virshup, D. M. (2007). Post-translational modifications regulate the ticking of the circadian clock. *Nature Reviews Molecular Cell Biology*, 8(2):139–148.

[10] Gerdes, K. (1988). The parb (hok/sok) locus of plasmid r1: a general purpose plasmid stabilization system. *Nature Biotechnology*, 6(12):1402–1405.

[11] Hsiao, V., de los Santos, E. L., Whitaker, W. R., Dueber, J. E., and Murray, R. M. (2014). Design and implementation of a biomolecular concentration tracker. *ACS synthetic biology*, 4(2):150–161.

[12] Kinderman, F. S., Kim, C., von Daake, S., Ma, Y., Pham, B. Q., Spraggon, G., Xuong, N.-H., Jennings, P. A., and Taylor, S. S. (2006). A dynamic mechanism for akap binding to rii isoforms of camp-dependent protein kinase. *Molecular cell*, 24(3):397–408.

[13] Lestas, I., Vinnicombe, G., and Paulsson, J. (2010). Fundamental limits on the suppression of molecular fluctuations. *Nature*, 467(7312):174–178.

[14] Liu, C. C., Qi, L., Lucks, J. B., Segall-Shapiro, T. H., Wang, D., Mutalik, V. K., and Arkin, A. P. (2012). An adaptor from translational to transcriptional control enables predictable assembly of complex regulation. *Nature methods*, 9(11):1088–1094.

[15] Qian, Y. and Del Vecchio, D. (2017). Realizing "integral control" in living cells: How to overcome leaky integration due to dilution? *bioRxiv*.

[16] Sharma, U. K. and Chatterji, D. (2008). Differential mechanisms of binding of anti-sigma factors escherichia coli rsd and bacteriophage t4 asia to e. coli rna polymerase lead to diverse physiological consequences. *Journal of bacteriology*, 190(10):3434–3443.

[17] Van Melderen, L., Thi, M. H. D., Lecchi, P., Gottesman, S., Couturier, M., and Maurizi, M. R. (1996). Atp-dependent degradation of ccda by lon protease effects of secondary structure and heterologous subunit interactions. *Journal of Biological Chemistry*, 271(44):27730–27738.

[18] Walton, S. P., Stephanopoulos, G. N., Yarmush, M. L., and Roth, C. M. (2002). Thermodynamic and kinetic characterization of antisense oligodeoxynucleotide binding to a structured mrna. *Biophysical journal*, 82(1):366–377.